JOURNAL OF AGRICULTURAL AND FOOD CHEMISTRY

pubs.acs.org/JAFC Article

Metabolic Engineering of *Escherichia coli* for Bioproduction of (*R*)-3-Hydroxybutyric Acid through a Three-Pronged Approach

Jinhong Chen,[⊥] Likun Guo,[⊥] Ying Zhang, Mohan Zhao, Meijie Li, Zhe Zhao, Qingsheng Qi, Mo Xian, Min Liu,* and Guang Zhao*

Cite This: https://doi.org/10.1021/acs.jafc.4c04123 Read Online

ACCESS | Metrics & More | Article Recommendations | Supporting Information

ABSTRACT: (*R*)-3-Hydroxybutyric acid (*R*-3HB) is an important chiral chemical with extensive applications in the agricultural, food, and chemical industries. The synthesis of *R*-3HB by microbial fermentation is of interest due to its remarkable stereoselectivity and economy. However, the low production of *R*-3HB failed to meet the needs of large-scale industrial production. In this study, an engineered strain for the efficient biosynthesis of *R*-3HB was constructed through a three-pronged approach encompassing biosynthetic pathway optimization, engineering of NADPH regenerators, and central metabolism regulation. The engineered strain Q5081 produced 75.7 g/L *R*-3HB, with a productivity of 1.26 g/L/h and a yield of 0.34 g/g glucose in fed-batch fermentation, showing the highest reported titer and productivity of *R*-3HB to date. We also performed transcriptome sequencing and annotation to illustrate the mechanism underlying the enhanced *R*-3HB production. The systematic metabolic engineering by a three-pronged approach demonstrated the feasibility of improving the biosynthesis, and the engineered strain Q5081 has the potential for widespread applications in the industrial production of *R*-3HB.

KEYWORDS: *(R)-3-hydroxybutyric acid, systematic metabolic engineering, transcriptome, NADPH, Escherichia coli*

1. INTRODUCTION

Chiral molecules are widely used as building blocks for the synthesis of many high-value compounds. The chirality of a molecule can usually directly determine its activity and effectiveness.[1,2] Thus, the acquisition of a chiral molecule with high optical purity is of significant interest. The synthesis of stereoisomers through chemical processes is not economically feasible with the harsh condition control and inevitable formation of byproducts.[3] In contrast, the application of a bioprocess has attracted more attention due to its high stereoselectivity and economy.[4] The biosynthesis of (*R*)-3-hydroxybutyric acid (*R*-3HB) is a typical example. *R*-3HB is a monomer of poly(3-hydroxybutyric acid) (P3HB). P3HB is one of the most attractive biodegradable polyesters since it has properties similar to those of polypropylene and can rapidly biodegrade under various environmental conditions.[5,6] These characteristics enable P3HB with high demands in food packaging and agricultural films. Furthermore, *R*-3HB can be used as a valuable precursor for the synthesis of antibiotics, vitamins, pheromones, and flavor compounds.[7−10] Pheromones have been demonstrated to be a new environmentally safe strategy for controlling agricultural pest.[11] Flavor compounds are usually used to impart a desired taste in beverages and foods.[12] In summary, *R*-3HB is a valuable chemical with extensive applications in agricultural and food industries.

R-3HB was mainly produced by two typical approaches. In one route, P3HB is synthesized and then depolymerized into 3HB by enzymatic catalysis. The second route is the direct synthesis of 3HB through CoA removal (Supporting Figure 1). The degradation process is too expensive and complicated to be suitable for industrial applications.[13] Therefore, *R*-3HB bioproduction studies have focused on the direct synthesis in recent years. The reported direct synthetic pathways of *R*-3HB are listed in Supporting Figure 1. First, two acetyl-CoA molecules are condensed into acetoacetyl-CoA by the catalysis of *β*-ketothiolase (PhaA), and then, NADPH-dependent acetoacetyl-CoA reductase (PhaB) catalyzes the conversion of acetoacetyl-CoA to (*R*)-3-hydroxybutyryl-CoA (*R*-3HB-CoA). *R*-3HB-CoA can be transformed to (*R*)-3-hydroxybutyryl phosphate (*R*-3HB-P) by phosphortransbutyrylase (Ptb) and then butyrate kinase (Buk) catalyzes the conversion of *R*-3HB-P to *R*-3HB. Gao et al. constructed the BuK pathway, producing 12 g/L *R*-3HB in fed-batch fermentation after 48 h.[4] *R*-3HB can also be generated from *R*-3HB-CoA using a propionyl-CoA transferase (PCT), which transfers the CoA moiety of *R*-3HB-CoA to other short-chain organic acid. An engineered *Escherichia coli* strain achieved 1.02 g/L *R*-3HB with syngas-derived acetate as the sole carbon source using the PCT pathway.[6] In addition, *R*-3HB-CoA is also directly converted to *R*-3HB by the catalysis of thioesterase (TesB), and the highest reported titer was 16.3 g/L in nitrogen-limited fed-batch cultivations by this pathway.[14]

Although researchers have made some great efforts, the limited titer of *R*-3HB has yet to successfully reach the need for

Received: May 10, 2024
Revised: July 11, 2024
Accepted: July 12, 2024

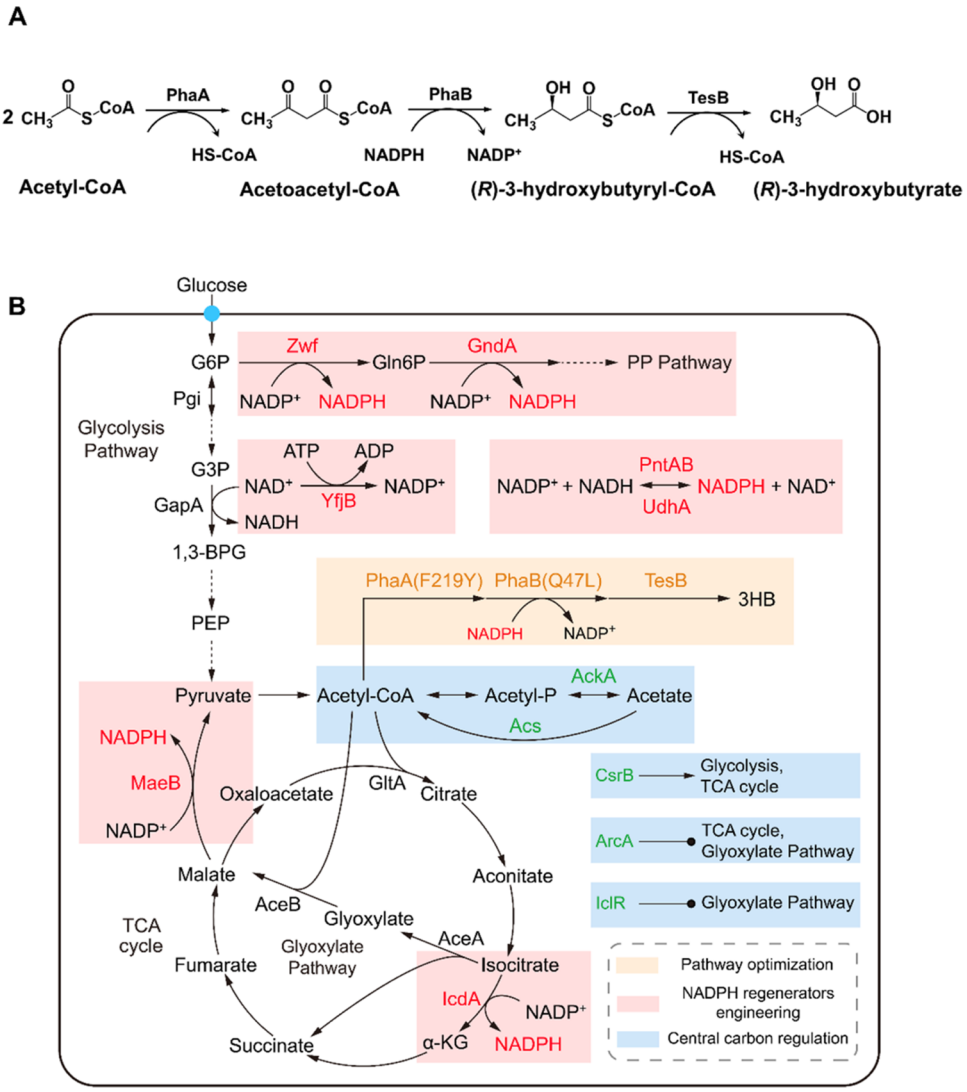

Figure 1. Metabolic engineering of *E. coli* for bioproduction of *R*-3HB. (A) Biosynthetic pathway of *R*-3HB. (B) Three-pronged approach includes pathway optimization, engineering of NADPH regenerators, and central metabolic network regulation. PhaA, *β*-ketothiolase; PhaB, acetoacetyl-CoA reductase; TesB, thioesterase; Zwf, glucose-6-phosphate dehydrogenase; GndA, 6-phosphogluconate dehydrogenase; IcdA, isocitrate dehydrogenase; MaeB, malic enzyme; PntAB, membrane-bound transhydrogenase; UdhA, soluble transhydrogenase; YfjB, native NAD kinase; Acs, acetyl-CoA synthase; and AckA, acetate kinase.

large-scale industrial production. Comparing the above three pathways to synthesize *R*-3HB, TesB catalyzes the direct removal of CoA in a relatively simple way, and the highest reported titer of *R*-3HB was produced by the TesB pathway. Therefore, we constructed the TesB pathway for *R*-3HB production and achieved an efficient engineered *E. coli* strain through a three-pronged approach including pathway optimization, engineering of NADPH regenerators, and central metabolic network regulation (Figure 1). The systematic metabolic engineering obviously improved *R*-3HB production, and the engineered strain will have great potential for commercial applications.

2. MATERIALS AND METHODS

2.1. Constructions of Plasmids and Strains. All primers used in this study are listed in Supporting Table 1, and all plasmids and strains used in this study are listed in Table 1. The *pcs′* gene (encoding the residues 1−856) from *Chloroflexus aurantiacus* and *phaA* and *phaB* genes from *Ralstonia eutropha* H16 were synthesized in BGI Genomics Co., Ltd. (Beijing, China). Other genes were cloned from *E. coli* BL21(DE3). *E. coli* DH5*α* was used as the host for gene cloning, and *E. coli* BL21(DE3) was used as the host for protein expression and *R*-3HB production. The *E. coli χ*7213 strain containing the suicide vector was used for conjugation and transformation.[15] All of the recombinant plasmids were constructed using standard restriction cloning and sequenced for confirmation. Chromosomal genes were deleted via P_1 vir-mediated transduction, and the donor strains were purchased from the Keio collection.[16] The T_7-lacO sequence (TAATACGACTCACTATAGGGGAATTGTGAGCGG ATAACAATTCC) was inserted into the chromosome before the *csrB* gene using suicide plasmid pRE112-mediated homologous recombination for inducing the overexpression of *csrB*.

2.2. Protein Expression and Gel Electrophoresis Analysis. Single colonies of *E. coli* cells harboring different plasmids were grown overnight at 37 °C and cultivated in LB medium with appropriate antibiotics.

The seed culture was diluted 1:50 into fresh fermentation medium of *R*-3HB and further incubated under the same conditions. When the OD_{600} of the culture reached about 0.8, IPTG was added to 25 μM for inducing protein expression, and the cells were further cultivated for 12 h at 30 °C. Cells were collected by centrifugation, washed twice, resuspended in phosphate buffered saline (pH 7.5), and disrupted by

https://doi.org/10.1021/acs.jafc.4c04123
J. Agric. Food Chem. XXXX, XXX, XXX−XXX

Table 1. Strains and Plasmids Used in This Study

strains and plasmids	description	source
strains		
E. coli DH5α	F$^-$ *supE*44 Δ*lacU*169 (ϕ80 *lacZ* Δ*M15*) *hsdR*17 *recA*1 *endA*1 *gyrA*96 *thi*-1 *relA*1	invitrogen
E. coli BL21(DE3)	F$^-$ *ompT gal dcm lon hsdSB* (rB$^-$ mB$^-$) λ(DE3)	invitrogen
E. coli χ7213	*thi*-1 *thr*-1 *leu*B6 *gln*V44 *fhu*A21 *lac*Y1 *rec*A1 *RP4*-2-Tc: Mu λ*pir* Δ*asd*A4 Δ*zhf*-2: *Tn*10	15
3HB-producing strains		
Q4504	*E. coli* BL21(DE3)/pET-*tesB-phaA-phaB*	this study
Q4505	*E. coli* BL21(DE3)/pET-*yciA-phaA-phaB*	this study
Q4508	*E. coli* BL21(DE3)/pET-*prpE-phaA-phaB*	this study
Q4509	*E. coli* BL21(DE3)/pET-*pcs′-phaA-phaB*	this study
Q5065	*E. coli* BL21(DE3)/pET-*tesB-phaA-phaB* (Q47L)	this study
Q5066	*E. coli* BL21(DE3)/pET-*tesB-phaA-phaB* (T173S)	this study
Q5067	*E. coli* BL21(DE3)/pET-*tesB-phaA-phaB* (Q47L/T173S)	this study
Q5068	*E. coli* BL21(DE3)/pET-*tesB-phaA*(F219Y)-*phaB*(Q47L)	this study
Q5048	*E. coli* BL21(DE3)/pET-*tesB-phaA-phaB*/pA-*zwf*	this study
Q5049	*E. coli* BL21(DE3)/pET-*tesB-phaA-phaB*/pA-*gndA*	this study
Q5050	*E. coli* BL21(DE3)/pET-*tesB-phaA-phaB*/pA-*icdA*	this study
Q5051	*E. coli* BL21(DE3)/pET-*tesB-phaA-phaB*/pA-*maeB*	this study
Q5052	*E. coli* BL21(DE3)/pET-*tesB-phaA-phaB*/pA-*yfjB*	this study
Q5053	*E. coli* BL21(DE3)/pET-*tesB-phaA-phaB*/pA-*pntAB*	this study
Q5054	*E. coli* BL21(DE3)/pET-*tesB-phaA-phaB*/pA-*udhA*	this study
Q5058	*E. coli* BL21(DE3)/pET-*tesB-phaA-phaB*/pA-*pntAB-yfjB*	this study
Q5070	*E. coli* BL21(DE3) Δ*arcA*/pET-*tesB-phaA-phaB*	this study
Q5071	*E. coli* BL21(DE3) Δ*iclR*/pET-*tesB-phaA-phaB*	this study
Q5072	*E. coli* BL21(DE3) P_{T7} *csrB*/pET-*tesB-phaA-phaB*	this study
Q5073	*E. coli* BL21(DE3) Δ*ackA*/pET-*tesB-phaA-phaB*	this study
Q5075	*E. coli* BL21(DE3)/pET-*tesB-phaA-phaB*/pA-*acs*	this study
Q5076	*E. coli* BL21(DE3) Δ*iclR* P_{T7} *csrB*/pET-*tesB-phaA-phaB*	this study
Q5077	*E. coli* BL21(DE3) Δ*iclR*/pET-*tesB-phaA-pha* /pA-*acs*	this study
Q5078	*E. coli* BL21(DE3) P_{T7} *csrB*/pET-*tesB-phaA-phaB*/pA-*acs*	this study
Q5079	*E. coli* BL21(DE3) Δ*iclR* P_{T7} *csrB*/pET-*tesB-phaA-phaB* /pA-*acs*	this study
Q5080	*E. coli* BL21(DE3)/pET-*tesB-phaA*(F219Y)-*phaB*(Q47L) /pA-*pntAB-yfjB*	this study
Q5081	*E. coli* BL21(DE3) Δ*iclR* P_{T7} *csrB*/pET-*tesB-phaA*(F219Y)-*phaB*(Q47L)/pA-*pntAB-yfjB-acs*	this study
protein expression strains		
Q5605	*E. coli BL21(DE3)/pA-zwf*	this study
Q5606	*E. coli* BL21(DE3)/pA-*gndA*	this study
Q5607	*E. coli* BL21(DE3)/pA-*icdA*	this study
Q5608	*E. coli* BL21(DE3)/pA-*maeB*	this study
Q5609	*E. coli* BL21(DE3)/pA-*yfjB*	this study
Q5610	*E. coli* BL21(DE3)/pA-*pntAB*	this study
Q5611	*E. coli* BL21(DE3)/pA-*udhA*	this study
Q5612	*E. coli* BL21(DE3)/pET-*tesB*	this study
Q5613	*E. coli* BL21(DE3)/pET-*yciA*	this study
Q5614	*E. coli* BL21(DE3)/pET-*prpE*	this study
Q5615	*E. coli* BL21(DE3)/pET-*pcs′*	this study
plasmids		
pETDuet1	rep_{pBR322} Amp^R *lacI* P_{T7}	invitrogen
pET-*tesB-phaA-phaB*	rep_{pBR322} Amp^R *lacI* P_{T7} *tesB* P_{T7} *phaA phaB*	this study
pET-*yciA-phaA-phaB*	rep_{pBR322} Amp^R *lacI* P_{T7} *yciA* P_{T7} *phaA phaB*	this study
pET-*prpE-phaA-phaB*	rep_{pBR322} Amp^R *lacI* P_{T7} *prpE* P_{T7} *phaA phaB*	this study
pET-*pcs′-phaA-phaB*	rep_{pBR322} Amp^R *lacI* P_{T7} *pcs′* P_{T7} *phaA phaB*	this study
pET-*tesB-phaA-phaB* (Q47L)	rep_{pBR322} Amp^R *lacI* P_{T7} *tesB* P_{T7} *phaA phaB*(Q47L)	this study
pET-*tesB-phaA-phaB* (T173S)	rep_{pBR322} Amp^R *lacI* P_{T7} *tesB* P_{T7} *phaA phaB*(T173S)	this study
pET-*tesB-phaA-phaB* (Q47L/T173S)	rep_{pBR322} Amp^R *lacI* P_{T7} *tesB* P_{T7} *phaA phaB*(Q47L/T173S)	this study
pET-*tesB-phaA* (F219Y)-*phaB*(Q47L)	rep_{pBR322} Amp^R *lacI* P_{T7} *tesB* P_{T7} *phaA*(F219Y) *phaB*(Q47L)	this study
pET-*tesB*	rep_{pBR322} Amp^R *lacI* P_{T7} *tesB*	this study
pET-*yciA*	rep_{pBR322} Amp^R *lacI* P_{T7} *yciA*	this study
pET-*prpE*	rep_{pBR322} Amp^R *lacI* P_{T7} *prpE*	this study
pET-*pcs′*	rep_{pBR322} Amp^R *lacI* P_{T7} *pcs′*	this study
pACYCDuet1	rep_{p15A} Cm^R *lacI* P_{T7}	invitrogen
pA-*zwf*	rep_{p15A} Cm^R *lacI* P_{T7} *zwf*	this study
pA-*gndA*	rep_{p15A} Cm^R *lacI* P_{T7} *gndA*	this study

https://doi.org/10.1021/acs.jafc.4c04123
J. Agric. Food Chem. XXXX, XXX, XXX−XXX

Table 1. continued

strains and plasmids	description	source
pA-*icd*	rep_{p15A} Cm^R *lacI* P_{T7} *icd*	this study
pA-*maeB*	rep_{p15A} Cm^R *lacI* P_{T7} *maeB*	this study
pA-*yfjB*	rep_{p15A} Cm^R *lacI* P_{T7} *yfjB*	this study
pA-*pntAB*	rep_{p15A} Cm^R *lacI* P_{T7} *pntA pntB*	this study
pA-*udhA*	rep_{p15A} Cm^R *lacI* P_{T7} *udhA*	this study
pA-*pntAB-yfjB*	rep_{p15A} Cm^R *lacI* P_{T7} *pntA pntB yfjB*	this study
pA-*pntAB-yfjB-acs*	rep_{p15A} Cm^R *lacI* P_{T7} *pntA pntB yfjB* P_{T7} *acs*	this study
pA-*acs*	rep_{p15A} Cm^R *lacI* P_{T7} *acs*	this study

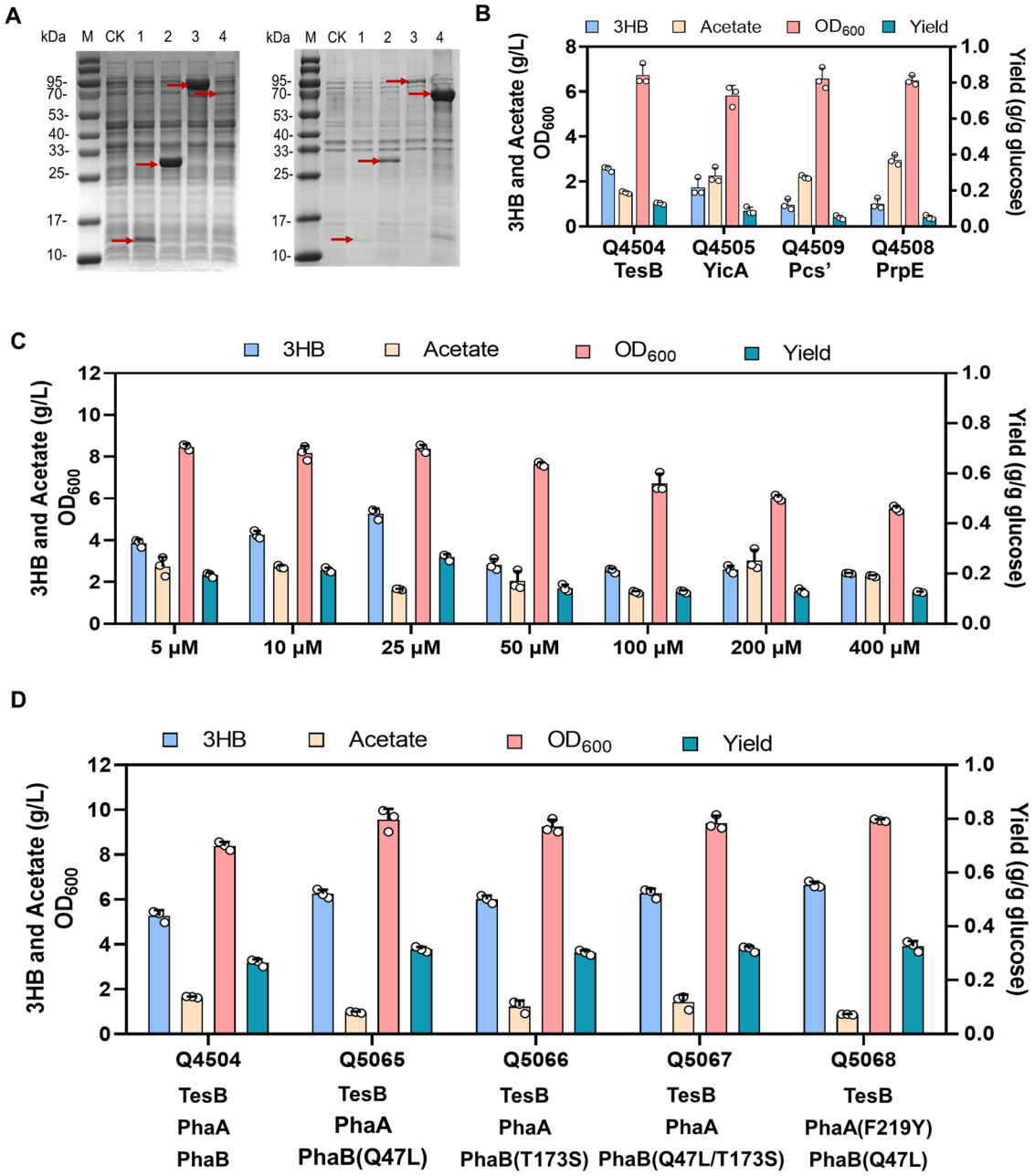

Figure 2. Synthetic pathway optimization of *R*-3HB. (A) Supernatant (left) and centrifuged deposits (right) of the cell lysates from different protein expression strains were analyzed by Coomassie brilliant blue-stained SDS-PAGE. Lane M, protein molecular mass marker; Lane CK, cell lysates from *E. coli* BL21(DE3) containing pETDuet1; Lane 1, cell lysates from Q5613 (YciA-OE); Lane 2, cell lysates from Q5612 (TesB-OE); Lane 3, cell lysates from Q5615 (Pcs′-OE); Lane 4, cell lysates from Q5614 (PrpE-OE); and OE, overexpression. (B) *R*-3HB production to compare different thioesterases for converting *R*-3HB-CoA to *R*-3HB, the concentration of IPTG was 100 μM. (C) *R*-3HB production of Q4504 to compare different concentrations of IPTG. (D) *R*-3HB production to compare different mutants of PhaA and PhaB. The detail results are also shown in Supporting Table 2.

https://doi.org/10.1021/acs.jafc.4c04123
J. Agric. Food Chem. XXXX, XXX, XXX−XXX

high pressure. The cell lysates were centrifuged, and the proteins in the supernatant were quantified using a BCA protein assay kit (Pierce). The centrifuged deposits were also resuspended in the same volume of phosphate buffered saline. All the samples were analyzed by 12% sodium dodecyl sulfate-polyacrylamide gel electrophoresis (SDS-PAGE) according to standard protocols.

2.3. Shake-Flask Cultivation. To evaluate the ability of *R*-3HB production in different strains, shake-flask experiments were performed in a triplicate series of 250 mL Erlenmeyer flasks containing appropriate antibiotics. Strains were cultivated overnight at 37 °C in LB broth and 1:50-diluted into 50 mL of fresh broth, including 14 g/L $K_2HPO_4·3H_2O$, 5.2 g/L KH_2PO_4, 1 g/L NaCl, 1 g/L NH_4Cl, 0.25 g/L $MgSO_4·7H_2O$, 0.2 g/L yeast extract, and 20 g/L glucose. When OD_{600} reached about 0.8, 25 μM IPTG was added, and the cells were further cultivated for 48 h at 30 °C.

2.4. Fed-Batch Fermentation. The fed-batch cultures were carried out in a 5 L fermenter containing 2 L of fermenting medium (9.8 g/L $K_2HPO_4·3H_2O$, 2.1 g/L citric acid·H_2O, 0.3 g/L ferric ammonium citrate, 3.0 g/L $(NH_4)_2SO_4$), 0.5 g/L $MgSO_4$, 0.018 g/L $CaCl_2·2H_2O$, 20 g/L glucose, and 1000× trace elements, including 6 g/L $FeSO_4·7H_2O$, 2 g/L H_3BO_3, 2 g/L $MnCl_2·4H_2O$, 0.8 g/L $(NH_4)_6No_7O_{24}·4H_2O$, and 0.2 g/L$CuSO_4·5H_2O$. During the fermentation process, pH was controlled automatically at 7.0 by addition of ammonia−water and 2.5 M H_2SO_4. 50% (w/w) glucose was begun to feed when the 20 g/L initial glucose was deleted. The dissolved oxygen (DO) level was maintained at 20 ± 1% by automatically adjusting the stirring rate from 300 to 700 rpm. When the OD_{600} of cells reached about 16, 25 μM IPTG was added to the culture and further incubated for 60 h at 30 °C for *R*-3HB production.

2.5. Analytical Methods. The cell growth was assayed by measuring the OD_{600} using a spectrophotometer (U-2900; Hitachi). The glucose concentration was detected by an SBA-40ES biological sensing analyzer (Institute of Biology, Shandong Academy of sciences, China). Metabolites were analyzed by a high-performance liquid chromatography (HPLC) system equipped with an HPX-87H column (Bio-Rad, Hercules, CA) (300 mm × 7.8 mm). All samples were filtered through a 0.22 μm syringe filter. 5 mM H_2SO_4 was used as the eluent at 0.6 mL/min, and the oven temperature was maintained at 65 °C. NADPH and $NADP^+$ were extracted from the cells after IPTG induction for 12 h and determined using the Coenzyme II NADP(H) Content Assay Kit (Solarbio, Beijing, China).

2.6. Transcriptomic Analysis. *E. coli* cells were collected after 12 h of IPTG induction, total RNA was extracted, and the RNA integrity was assessed using the RNA Nano 6000 Assay Kit and the Bioanalyzer 2100 system (Agilent Technologies, CA). Libraries were constructed using the NEBNext UltraTM RNA Library Prep Kit for Illumina (NEB) according to the manufacturer's recommendations. These libraries were then sequenced at Beijing Novogene Bioinformatics Technology Co., Ltd. The reads containing the adapter and poly-N and low-quality reads were filtered. The clean reads were aligned with the genome of *E. coli* BL21(DE3). Differential expression analysis was performed using the DESeq2 R package (1.16.1). Genes with an adjusted *P*-value of <0.05 found by DESeq2 were assigned as differentially expressed.

3. RESULTS AND DISCUSSION

3.1. Construction and Optimization of the *R*-3HB Biosynthetic Pathway. For *R*-3HB production, *phaA* and *phaB* genes were cloned to pETDuet-1 and overexpressed in the *E. coli* BL21(DE3) strain. Given the broad substrate specificity, two native *E. coli* thioesterases encoded by *tesB* and *yciA* as well as two CoA-synthetases encoded by *prpE* and *pcs′* were selected as candidates for catalyzing the conversion of *R*-3HB-CoA to *R*-3HB. TesB has relatively broad substrate specificity that mediates the irreversible one-step hydrolysis of *R*-3HB-CoA to *R*-3HB.[17] Similar to TesB, YciA has exhibited substrate specificity and significant catalytic efficiency for many short- to medium-chain acyl-CoA intermediates, including 3HB-CoA, acetyl-CoA, and acetoacetyl-CoA.[18] These two thioesterases, TesB and YciA, were previously used for the *R*-3HB bioproduction.[8,14] Propionyl-CoA synthase (Pcs) from *C. aurantiacus* is a trifunctional enzyme, consisting of an acyl-CoA ligase, an enoyl-CoA hydratase, and an enoyl-CoA reductase domain.[19] The acyl-CoA ligase domain of Pcs (residues 1−856) showed high sequence similarities to acetyl-CoA and some short fatty acid acyl-CoA synthetases[19,20] and was referred to as Pcs′ and tested in this study. The propionyl-CoA synthetase (PrpE) from *E. coli* catalyzes the formation of propinoyl-CoA, which is the first reaction of propionate catabolism.[21] Pcs′ and PrpE are short-chain acyl-CoA synthetases, and they might be able to catalyze the reverse reaction of CoA removal. To discover a new type of enzyme for 3HB biosynthesis, these two enzymes were tested in this study, although their CoA removal activity has not been reported.

The four candidate genes were overexpressed and compared for their ability to produce *R*-3HB. The proteins of TesB, YciA, and *Pcs′* mainly existed in the supernatant of the cell lysate, while PrpE protein was mainly present in inclusion bodies (Figure 2A). Overexpression of *tesB* resulted in the highest *R*-3HB titer and yield as well as the lowest accumulation of acetate, the main byproduct during fermentation (Figure 2B). The titer of *R*-3HB in Q4504 was 1.48 times higher than that in Q4505, and the acetate concentration in Q4504 was decreased to 67.1%. Our results demonstrated that the overexpression of TesB is more beneficial to the production of *R*-3HB than the overexpression of YciA in *E. coli*. This may be due to the higher soluble expression level of TesB compared to that of YciA (Figure 2A). In addition, the titers of *R*-3HB in Q4508 and Q4509 were significantly lower compared to those of Q4504 and Q4505. According to these results, it cannot determine whether the native *E. coli* thioesterase in the genome or these two enzymes perform the function of removing CoA. The results underline the importance of evaluating the effects of thioesterases on *R*-3HB production in specific strains, cultivation conditions, and synthetic pathways.

According to the above results, the TesB pathway for *R*-3HB synthesis was constructed (Figure 1A). However, only 2.56 g/L *R*-3HB was obtained under this cultivation condition (Figure 2B). As the concentration of the inducer IPTG determines the expression level of heterologous proteins in the *R*-3HB pathway, we compared the production *R*-3HB of Q4504 at different concentrations of IPTG, ranging from 5 to 400 μM. High concentrations of IPTG induction suppressed *R*-3HB synthesis and cell biomass, and induction with 25 μM IPTG achieved the highest titer and yields of 5.27 and 0.27 g/g glucose, respectively (Figure 2C). Consequently, the concentration of IPTG was adjusted from 100 to 25 μM for subsequent experiments.

Optimizing the activities of the two key enzymes of PhaA and PhaB may further improve the production of *R*-3HB. In previous study, two PhaB mutants, Q47L and T173S, were selected by directed evolution and a P(3HB) concentration-based screening system, exhibiting significantly increased enzyme activity and P(3HB) accumulation.[22] Thus, we compared the production of *R*-3HB between the strains of Q5065, Q5066, and Q5067. The PhaB mutants indeed improved the titer and yield of *R*-3HB. However, the double mutant Q5067 did not show better effects than the single mutants (Figure 2D). Among them, Q5065 accumulated a relatively lower acetate concentration. In addition, a previous

https://doi.org/10.1021/acs.jafc.4c04123
J. Agric. Food Chem. XXXX, XXX, XXX−XXX

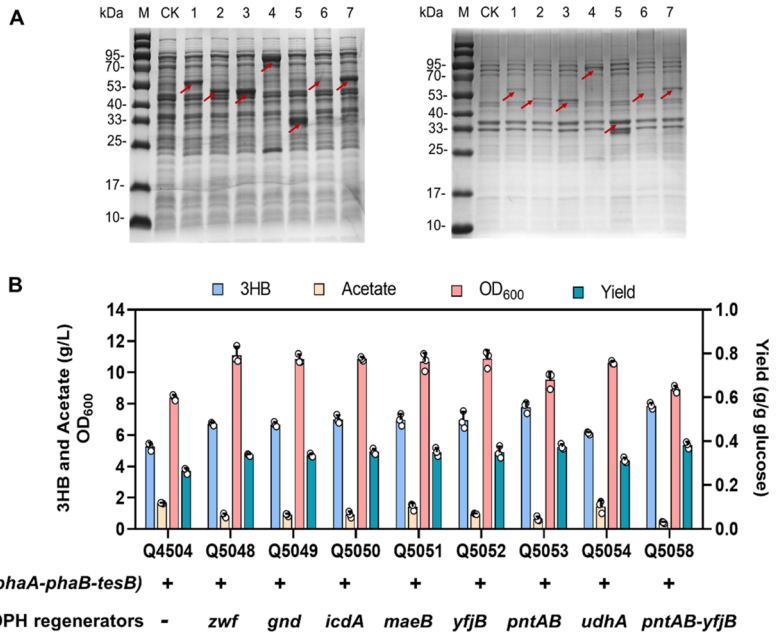

Figure 3. Engineering of NADPH regenerators for *R*-3HB production. (A) Supernatant (left) and centrifuged deposits (right) of the cell lysates from different protein expression strains were analyzed by Coomassie brilliant blue-stained SDS-PAGE. Lane M, protein molecular mass marker; Lane CK, cell lysates from *E. coli* BL21(DE3) containing pACYCDuet1; Lane 1, cell lysates from Q5605 (Zwf-OE); Lane 2, cell lysates from Q5606 (GndA-OE); Lane 3, cell lysates from Q5607 (IcdA-OE); Lane 4, cell lysates from Q5608 (MaeB-OE); Lane 5, cell lysates from Q5609 (YfjB-OE); Lane 6, cell lysates from Q5610 (PntAB-OE); Lane 7, cell lysates from Q5611(UdhA-OE); and OE, overexpression. (B) *R*-3HB production to compare different engineerings of NADPH regenerators. The detailed results are also shown in Supporting Table 2.

study has described the crystal structure of PhaA from *R. eutropha* in complex with CoA.[23] This study revealed that Phe219 played an important role in binding the ADP moiety through its marked hydrophobicity. The F219Y mutant improved the enzyme activity more than 2 times, probably because the water-mediated hydrogen bond between the pyrophosphate group and tyrosine residue enables the substrate to bind the enzyme more tightly.[23] Based on these results, we constructed a strain Q5068 carrying PhaA(F219Y) and PhaB (Q47L) mutants, improving the *R*-3HB production from 5.27 g/L in Q4504 to 6.65 g/L and decreasing acetate accumulation from 1.65 to 0.87 g/L.

In conclusion, pathway optimization, including evaluation and activity enhancement of key enzymes, is crucial for improving the production of desired chemicals, due to the varying effects of a candidate in the specific strains, synthetic pathways, and growth conditions. Furthermore, the concentration and yield of *R*-3HB were improved by more than 2-fold by concentration optimization of the inducer (Figure 2C). Therefore, process control and optimization are also necessary in the microbial fermentation. After pathway optimization, we finally constructed the TesB pathway for *R*-3HB production by overexpression of *phaA*(F219Y), *phaB*(Q47L), and *tesB* and determined the appropriate concentration of the inducer IPTG.

3.2. Engineering of NADPH Regenerators. Efficient availability of NADPH is one of the factors constraining the NADPH-dependent biotransformation processes of many value-added chemicals.[24,25] In the *R*-3HB synthetic pathway, PhaB catalyzes the NADPH-dependent reduction of acetoacetyl-CoA. Thus, engineering of NADPH regenerators may enhance the production of *R*-3HB. The transhydrogenase system, pentose phosphate (PP) pathway, and tricarboxylic acid cycle (TCA) are the major sources of NADPH[26] (Figure 1B). The genes of *zwf*, *gndA*, *icdA*, *maeB*, *yfjB*, *pntAB*, and *udhA* from these three pathways were overexpressed with our constructed TesB pathway. All of these proteins were successfully expressed in the soluble form (Figure 3A), and overexpression of each protein did enhance *R*-3HB synthesis (Figure 3B). As NADPH is also a requirement for biomass synthesis,[27,28] engineering of NADPH generators may enhance the supply of NADPH and further increase the cell biomass (Figure 3B). In addition, the overexpression of these genes involved in NADPH generation also decreased the acetate accumulation probably because more acetyl-CoA, the shared precursor of both acetate and *R*-3HB, was consumed in the *R*-3HB synthesis.

More specifically, PntAB is an energy-dependent, membrane-bound transhydrogenase that catalyzes the transfer of a hydrogen ion from NADH to $NADP^+$. The strain Q5053 with *pntAB* overexpression showed the highest titer and yield of *R*-3HB, which were 1.53 and 1.48 times higher than those of the control strain Q4504, respectively. The other transhydrogenase UdhA is soluble and energy-independent, and its overexpression has been reported to increase the availability of NADPH in *E. coli*[29] even though UdhA mainly catalyzes the transfer of a hydrogen ion from NADPH to NAD^+.[30,31] The strain Q5054 with the overexpression of *udhA* caused a 1.16 times increase of the *R*-3HB titer compared to that of Q4504 (Figure 3B). In addition, the titer and yield of *R*-3HB in the strains of Q5050, Q5051, and Q5052 were very similar, which were higher than those of other strains except Q5053 (Figure 3B). Among them, YfjB is a native NAD kinase of *E. coli* that is known to have high specificity for NAD^+ compared to NADH.[32] The strain Q5052 with the overexpression of *yfjB* enhanced the *R*-3HB titer in our study, consistent with some previous results showing that its overexpression can increase NADPH-dependent biosynthesis of chemicals, such as PHB

https://doi.org/10.1021/acs.jafc.4c04123
J. Agric. Food Chem. XXXX, XXX, XXX−XXX

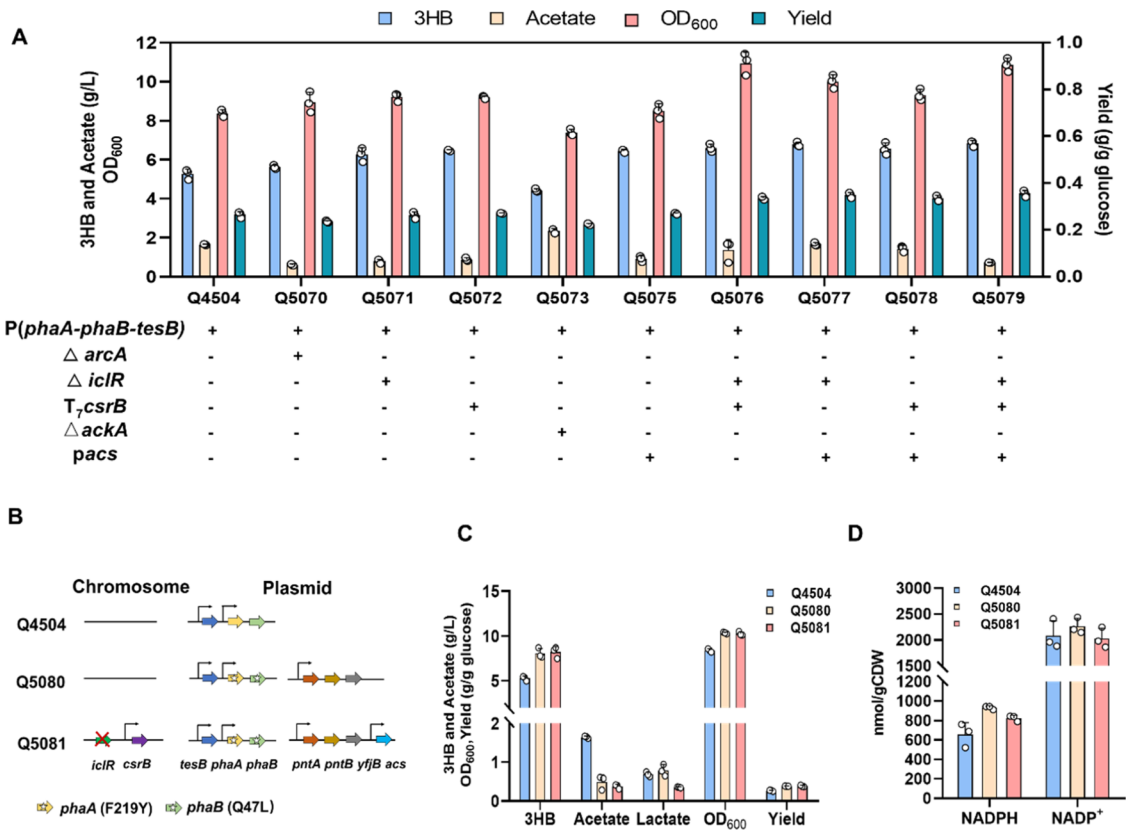

Figure 4. Strain optimization through global regulation of the central carbon metabolism. (A) *R*-3HB production to compare different genetic modifications. In the *E. coli* BL21(DE3) strain, *arcA*, *iclR*, and *ackA* were knocked out, the transcription of *csrB* was increased by insertion of a strong promoter P_{T7} ahead of this gene in the chromosome, and the *acs* gene was cloned into a plasmid under control of the IPTG-induced T_7 promoter. (B) Schematic representation of the strains of Q4504, Q5080, and Q5081 used in this study. (C) Comparison of *R*-3HB production in shake-flask cultivation between these three strains. (D) Intracellular concentrations of NADPH and $NADP^+$ were in these three strains. The detailed results are also shown in Supporting Table 2.

and thymidine.[26,33,34] As YfjB and PntAB can corporately convert NAD^+ into NADPH (Figure 1B), the genes of *pntAB* and *yfjB* were coexpressed with the TesB pathway in the strain Q5058, resulting in the increase of the *R*-3HB titer to 7.87 g/L and the decrease of acetate accumulation to an extremely low level of 0.41 g/L (Figure 3B).

NADPH, as an important cofactor, must be provided sufficiently to sustain efficient biotransformation processes and cellular metabolism. Hence, engineering NADPH regenerators for improving intracellular NADPH availability has been receiving more attention in recent years. Overexpression of transhydrogenases and $NADP^+$-dependent enzymes in central metabolism have been widely used for NADPH regeneration and achieved positive effects for NADPH-dependent biosynthesis of chemicals. However, engineering the enzymes involved in the redox balance of NADPH may result in some unknown metabolic perturbations.[26] How to minimize the side effects caused by engineering the NADPH regenerators and exploit some new strategies for a secure supply of NADPH will need more research.

3.3. Global Regulation of the Central Carbon Metabolism. The efficient bioproduction not only requires the optimization of the synthetic pathway but also relies on the rational manipulation of the endogenous metabolic network. As reported previously, manipulation of some genes involved in central carbon metabolism is beneficial to improving the production and yield of target chemicals of the engineered *E. coli* strain. The global regulator ArcA, along with ArcB, comprises a two-component system regulating the expression of numerous operons involved in carbon metabolism.[35] The transcription factor IclR represses the gene expression of the *aceBAK* operon, and deletion of *iclR* can activate the glyoxylate bypass.[36] Our previous studies have revealed that knockout of *arcA* and *iclR* can decrease the acetate accumulation and improve the productions of two important acetyl-CoA-derived chemicals, 3-hydroxypropionate (3HP) and phloroglucinol (PG).[37,38] CsrB is a noncoding small RNA that antagonizes CsrA-dependent translation inhibition by sequestering the binding of CsrA to mRNA.[39] Overexpression of *csrB* led to significant changes in protein and metabolite levels in the TCA cycle and glycolysis and further improved the productions of the free fatty acids and heterologous 1-butanol and isoprenoid.[39] On the metabolism of acetate, acetate kinase (AckA) catalyzes the conversion of acetyl phosphate to acetate, and acetyl-CoA synthase (Acs) can convert acetate to acetyl-CoA. Deletion of AckA and overexpression of Acs can disrupt the acetate synthetic pathway and promote acetate utilization.[35] Therefore, these five genetic modifications were selected for rational manipulation in this study.

We first constructed five strains carrying modification of a single gene. The genetic modifications did not impair the cell growth except the knockout of *ackA* (Figure 4A). Among them, *iclR* deletion, *csrB* overexpression, and *acs* overexpression significantly improved productions of *R*-3HB, and acetate

https://doi.org/10.1021/acs.jafc.4c04123
J. Agric. Food Chem. XXXX, XXX, XXX−XXX

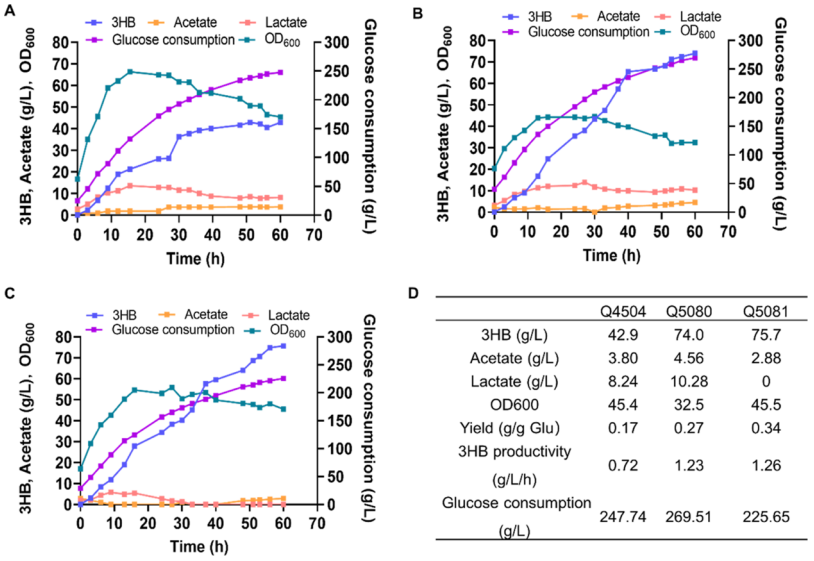

D

	Q4504	Q5080	Q5081
3HB (g/L)	42.9	74.0	75.7
Acetate (g/L)	3.80	4.56	2.88
Lactate (g/L)	8.24	10.28	0
OD600	45.4	32.5	45.5
Yield (g/g Glu)	0.17	0.27	0.34
3HB productivity (g/L/h)	0.72	1.23	1.26
Glucose consumption (g/L)	247.74	269.51	225.65

Figure 5. Bioproduction of *R*-3HB under fed-batch cultivation. Time profiles for the OD600, glucose consumption, acetate accumulation, *R*-3HB concentration, and yield of Q4504 (A), Q5080 (B) and Q5081 (C). (D) Production of *R*-3HB after IPTG induction for 60 h under fed-batch cultivation. The consumed glucose (g/L) = 20 g/L initial glucose + the feed glucose (g/L) − the residual glucose (g/L).

accumulations were decreased to 0.79, 0.89, and 0.92 g/L, respectively, as compared to the 1.65 g/L in the control strain Q4504 (Figure 4A). These three genetic modifications were combined randomly, and the strain Q5079 with three mutants of *iclR* deletion, *csrB* overexpression, and *acs* overexpression represented the highest titer and yield of 6.84 g/L and 0.36 g/g glucose, respectively. Meanwhile, the acetate concentration was decreased to 0.73 g/L (Figure 4A). By combining the functions of biosynthetic pathway optimization, engineering of NADPH regenerators, and central metabolism regulation, two engineered strains of Q5080 and Q5081 were constructed. The genes *tesB*, *phaA*(F219Y), and *phaB*(Q47L) in the *R*-3HB biosynthetic pathway and the genes of *pntAB* and *yfjB* involved in NADPH generation were simultaneously overexpressed, producing the Q5080 strain. The central metabolism regulation was further performed in the Q5080 strain through knockout of *iclR* and overexpression of *csrB* and *acs*, producing the Q5081 strain (Figure 4B). Surprisingly, there was no significant difference in the titer and yield of *R*-3HB between these two strains. *R*-3HB was accumulated to concentrations of 8.04 and 8.19 g/L, respectively, and the yields were both about 0.38 g/g glucose in Q5080 and Q5081 under shake-flask cultivation (Figure 4C). The acetate concentrations of Q5080 and Q5081 were 0.49 and 0.37 g/L, respectively, lower than that of 1.65 g/L in Q4504. However, the lactate accumulation in Q5080 was 0.79 g/L, 2.26 times higher than that of Q5081. In addition, we also compared the accumulation of NADPH and $NADP^+$ in these two engineered strains. The intracellular accumulations of NADPH in Q5080 and Q5081 strains were obviously higher than that of the control strain Q4504 due to the engineering of NADPH regenerators (Figure 4D).

These results demonstrated that it is possible to achieve a desirable performance in *R*-3HB biosynthesis through the three-pronged approach. The titer of *R*-3HB was improved from 2.56 to 8.19 g/L, the yield was enhanced from 0.13 to 0.38 g/g glucose, and the accumulation of the byproduct acetate was suppressed from 1.65 to 0.37 g/L. This systemic metabolic engineering enhanced the catalytic efficiency of key reactions, ensured an adequate supply of NADPH, and repressed the acetate overflow during the biosynthetic process of *R*-3HB. Contrary to our expectations, regulation of central carbon metabolism in the strain Q5080 did not achieve a significant improvement in *R*-3HB production. It seems that the acetate accumulation was already significantly decreased by the two strategies of biosynthetic pathway optimization and engineering of NADPH regenerators. Namely, the regulation of central carbon metabolism might be as significant as NADPH regenerations. In addition, the inability of shake-flask cultivation to exert the effects of global carbon metabolic regulation on improving the *R*-3HB synthesis may also be another reason for the similar *R*-3HB production and acetate accumulation between Q5080 and Q5081. The more comprehensive assessments of *R*-3HB production will be performed in the scale-up fermenting cultivation

3.4. *R*-3HB Production in Fed-Batch Fermentation.

According to the results of the shake-flask cultivation, the original strain Q4504 and its descendants Q5080 and Q5081 were grown under the fed-batch conditions in a 5 L fermenter to evaluate the robustness and suitability of these strains for the larger-scale production of *R*-3HB. The OD_{600}, glucose consumption, and the concentrations of *R*-3HB and acetate were monitored during the process of cultivation. After 20 h of IPTG induction, the OD_{600} of all these strains began to decline, whereas the concentration of *R*-3HB increased gradually with time (Figure 5A−C). After fermentation, Q5080 presented lower biomass accumulation than Q4504 and Q5081. The *R*-3HB titer of Q4504 was 42.9 g/L, with an average productivity of 0.72 g/(L·h) throughout the entire fermentation process. Those two optimized strains, Q5080 and Q5081, significantly improved the titer, yield, and productivity of *R*-3HB as compared to those of the control strain Q4504. The strain Q5080 produced 74.0 g/L *R*-3HB, with a productivity of 1.23 g/(L·h) and a yield of 0.27 g/g glucose. Interestingly, the strain Q5081 presented a higher *R*-3HB production of 75.7 g/L, whereas its glucose consumption was remarkably lower than that of the Q5080 strain, resulting in an enhanced yield of 0.34 g/g glucose (Figure 5D).

https://doi.org/10.1021/acs.jafc.4c04123
J. Agric. Food Chem. XXXX, XXX, XXX−XXX

Table 2. *R*-3HB Production in Microbes[a]

host	carbon source	cultivation	pathway	titer (g/L)	yield (g/g glucose)	productivity (g/L/h)	refs
E. coli BL21(DE3)	MM and glucose	fed-batch fermentation	TesB pathway	75.7	0.34	1.26	this study
E. coli BW25113	LB, glucose, and acetate	shake flask	PCT pathway	5.20		0.22	40
E. coli BW25113	syngas-derived acetate	shake flask	PCT pathway	1.02	0.26		6
E. coli DH5α	yeast extract and glucose	fed-batch fermentation	Buk pathway	12.0	0.20	0.25	4
E. coli MG1655	LB and glucose	shake flask	TesB pathway	3.63	0.41		10
E. coli BW25113	MM and glucose	fed-batch fermentation	TesB pathway	12.2	0.20	0.51	45
E. coli BL21	MM and glucose	fed-batch fermentation	TesB pathway	16.3	0.10	1.02	14

[a]MM: minimal medium.

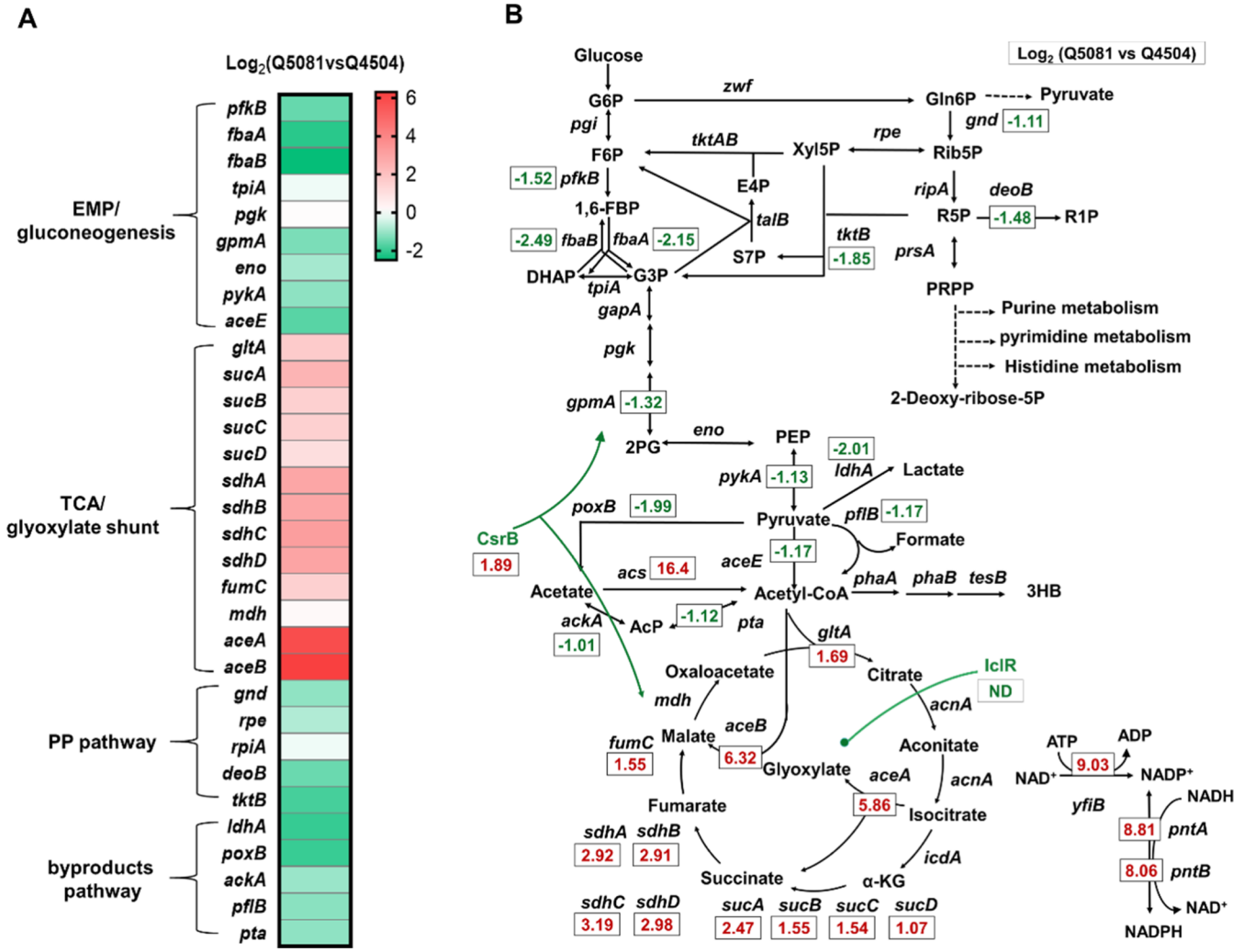

Figure 6. Regulation of central carbon metabolism on the gene transcription level in Q5081 as compared to Q4504. (A) Cluster analysis of differentially expressed genes (DEGs) related to the central carbon metabolism and byproduct synthetic pathways. (B) Sketch of DEGs in central metabolic pathways. G6P, glucose 6-phosphate; F6P, fructose 6-phosphate; 1,6-FBP, fructose 1,6-biphosphate; DHAP, dihydroxyacetone phosphate; G3P, glyceraldehyde 3-phosphate; 1,3-BPG, glycerate 1,3-biphosphate; 3PG, glycerate 3-phosphate; 2PG, glycerate 2-phosphate; PEP, phospho*enol*pyruvate; Ac-CoA, acetyl-CoA; AcP, acetyl phosphate; α-KG, α-ketoglutarate; Gln, gluconate; Gln6P, gluconate 6-phosphate; Rib5P, ribulose 5-phosphate; R5P, ribose 5-phosphate; R1P, ribose 1-phosphate; Xyl5P, xylulose 5-phosphate; E4P, erythrose 4-phosphate; S7P, sedoheptulose 7-phosphate; and PRPP, 5-phosphoribosyl-1-pyrophosphate.

Furthermore, the formation of byproducts, acetate and lactate, was also analyzed. After 60 h of fermentation, the concentrations of acetate in Q4504, Q5080, and Q5081 were relatively low, which accumulated at b3.80, 4.56, and 2.88 g/L, respectively (Figure 5D). However, the concentrations of lactate in both Q5080 and Q4504 were more than 13 g/L when the cells were in the exponential stage. The rapid cell growth in the exponential stage may reduce dissolved oxygen, leading to a significant accumulation of lactate. When the cell growth entered the stable stage, part of the lactate that accumulated in the early stage was consumed, and finally, the concentrations of lactate in Q4504 and Q5080 were reduced to 8.24 and 10.28 g/L, respectively. The accumulation of lactate in Q5081 remained below 5 g/L throughout the

https://doi.org/10.1021/acs.jafc.4c04123
J. Agric. Food Chem. XXXX, XXX, XXX−XXX

cultivation process and it was completely consumed at the end of fermentation. This may be the reason why Q5080 consumed more glucose but produced less cell biomass and lower *R*-3HB as compared to Q5081. In shake-flask cultivation, the cell growth of Q5080 has not yet been impaired due to the low accumulations of acetate and lactate, although their concentrations were also higher than those of Q5081 (Figure 4C). Therefore, the growth trends of Q5080 and Q5081 in fed-batch cultivation were inconsistent with the trends shown in shake-flask cultivation. These results suggested that global regulation of the central carbon metabolism can decrease the accumulation of byproducts and enhance the glucose conversion efficiency, although this function was not fully exerted in shake-flask cultivation.

Some previous reports have confirmed that cells harboring a CoA removal enzyme, PhaA and PhaB from *R. eutropha* H16, can produce *R*-3HB due to the enantioselectivity of PhaB,[10,40] whereas (*S*)-3-hydroxybutyryl-CoA (*S*-3HB-CoA) dehydrogenase (Hbd) from *R. eutropha* H16 or from *Clostridium acetobutylicum* ATCC824 catalyzes the conversion of acetoacetyl-CoA to *S*-3HB-CoA.[10,41] In our study, *phaA* (F219Y) and *phaB* (Q47L) from *R. eutropha* and *tesB* from *E. coli* BL21(DE3) were overexpressed for the synthesis of *R*-3HB. In order to confirm the chirality, 3HB produced by Q5081 was purified and analyzed by circular dichroism (CD). The CD spectra of the 3HB sample were essentially overlapped with those of the equimolar *R*-3HB standard, demonstrating that the 3HB produced by Q5081 was basically the *R*-form (Supporting Figure 2). The enantiopurity of *R*-3HB was about 96.7%, which is slightly lower than the previous reported data of 99.2%.[40] It is speculated that the purity of *R*-3HB separated from the Q5081 culture supernatant may affect testing of its optical purity.

Previously, Perez-Zabaleta et al. achieved the highest *R*-3HB titer of 16.3 g/L through decreasing the acetate formation, but the yield in that study was only about 0.10 g/g glucose (Table 2).[14] Tseng et al. reported a yield of *R*-3HB as high as 0.41 g/g glucose, which is not quite reliable as their strain was cultivated in LB medium supplemented with glucose and it is hard to tell whether the *R*-3HB is produced from glucose or the carbon source in LB medium.[10] In this study, we engineered *E. coli* BL21(DE3) through a three-pronged approach to generate a *R*-3HB-producing strain Q5081, which accumulated 75.7 g/L *R*-3HB in fed-batch fermentation, 4.64 times higher than the previous reported titer (Figure 5D). Furthermore, an *R*-3HB yield of 0.34 g/g glucose was achieved when the strain Q5081 was cultivated in minimal medium with glucose as the sole carbon source, showing superiority over previous strains. Currently, acetyl-CoA, the precursor for *R*-3HB biosynthesis, is produced from pyruvate with CO_2 release, resulting in a low theoretical yield of *R*-3HB. To further optimize the *R*-3HB production from glucose, a carbon-conserving pathway we constructed recently, named as the sedoheptulose-1,7-bisphosphatase cycle,[42] could be assembled with the *R*-3HB biosynthetic pathway. As this cycle directly converts 1 mol glucose into 3 mol AcP without CO_2 emission, it is possible to generate a recombinant strain presenting *R*-3HB yield higher than its native theoretical yield.

3.5. Transcriptome-Based Regulatory Mechanism Analysis. To elucidate the mechanism underlying the enhanced *R*-3HB production, transcriptome sequencing and annotation were performed to clarify the differences of gene expression between the control strain Q4504 and its descendant Q5081. A total of 763 differentially expressed genes (DEGs) were identified, with 314 genes upregulated and 449 genes downregulated in Q5081 as compared to Q4504 (Supporting Figure 3a). Furthermore, all of the identified DEGs were subjected to the Kyoto Encyclopedia of Genes and Genomes (KEGG) pathway enrichment analysis. This KEGG enrichment analysis revealed that the oxidative phosphorylation and carbon metabolism pathways in Q5081 underwent significant changes compared to the original strain Q4504 (Supporting Figure 3b). The gene expression levels of the central metabolic pathways, including the TCA cycle, glycolysis/gluconeogenesis, pentose phosphate, glyoxylate shunt, and byproduct synthetic pathway, were further analyzed for these two strains.

The gene expression levels of glycolysis/gluconeogenesis, pentose phosphate, and byproduct synthetic pathways in Q5081 were downregulated in varying degrees (Figure 6A,B). The *poxB* and *ldhA* genes involved in the formation of acetate and lactate from pyruvate were downregulated about fourfold in the Q5081 strain. Furthermore, the genes of *pflB* and *pta*, *ackA* for formate and acetate formation, were also downregulated about twofold. Thus, in the Q5081 strain, the transcriptions of byproduct synthetic genes were severely repressed through global regulation of the central carbon metabolism. In addition, the overexpression of the genes *yfiB* and *pntAB* led to a significant upregulation in the phosphorylation of NAD^+ and the transfer of hydrogen ions from NADH to $NADP^+$ in the Q5081 strain (Figure 6B). This elevation in transcription levels ensured an adequate supply of NADPH, crucial for the synthesis of *R*-3HB. It is noteworthy that the transcriptional levels of two genes involved in the glyoxylate shunt, *aceA* (encoding isocitrate lyase) and *aceB* (encoding isocitrate lyase), were increased by 58-fold and 80-fold in Q5081, respectively. Glyoxylate shunt is the main pathway for acetate assimilation.[43,44] Knockout of *iclR* can alleviate the transcriptional inhibition of the glyoxylate shunt, while overexpression of *acs* promotes the acetate assimilation to acetyl-CoA. Acetyl-CoA is the precursor for the biosynthesis of *R*-3HB, and acetate excretion can compete with the substrate for *R*-3HB. Therefore, these genetic modifications stimulated the utilization of acetate for net synthesis of biomass and *R*-3HB and reduced the useless depletion of the carbon source, ultimately resulting in improved bioproduction of *R*-3HB.

In conclusion, the Q5081 strain has successfully downregulated the synthetic pathways of byproducts, such as acetate, lactate, and formate through a global regulation of the central carbon metabolism. Coupled with the enhanced acetate assimilation and activated glyoxylate shunt, the Q5081 strain can overcome the acetate overflow, reduce the carbon loss, and improve the glucose conversion efficiency. Furthermore, biosynthetic pathway optimization and engineering of NADPH regenerators can improve the catalytic ability of key enzymes in the *R*-3HB synthetic pathway, ensure the sufficient supply of NADPH, and finally contribute to *R*-3HB bioproduction. The engineered strain Q5081 is expected to have a wide application potential for the large-scale production of *R*-3HB.

■ ASSOCIATED CONTENT

Supporting Information

The Supporting Information is available free of charge at https://pubs.acs.org/doi/10.1021/acs.jafc.4c04123.

https://doi.org/10.1021/acs.jafc.4c04123
J. Agric. Food Chem. XXXX, XXX, XXX−XXX

Primers used in this study, concentrations of *R*-3HB and acetate, OD600, yield of *R*-3HB in each strain under shake-flask cultivation, synthetic pathways of *R*-3HB from glucose, chiral analysis of 3HB produced from Q5081 by circular dichroism (CD), and overview of transcriptome analysis of Q5081 vs Q4504 (PDF)

AUTHOR INFORMATION

Corresponding Authors

Min Liu − *State Key Laboratory of Microbial Technology, Shandong University, Qingdao 266237, China;* orcid.org/0009-0007-0323-8291; Email: liumin88@email.sdu.edu.cn

Guang Zhao − *State Key Laboratory of Microbial Technology, Shandong University, Qingdao 266237, China;* orcid.org/0000-0003-0002-5972; Email: zhaoguang@sdu.edu.cn

Authors

Jinhong Chen − *State Key Laboratory of Microbial Technology, Shandong University, Qingdao 266237, China*

Likun Guo − *State Key Laboratory of Microbial Technology, Shandong University, Qingdao 266237, China*

Ying Zhang − *State Key Laboratory of Microbial Technology, Shandong University, Qingdao 266237, China*

Mohan Zhao − *Qingdao No. 2 Middle School, Qingdao 266061, China*

Meijie Li − *Energy-Rich Compound Production by Photosynthetic Carbon Fixation Research Center, Shandong Key Lab of Applied Mycology, College of Life Sciences, Qingdao Agricultural University, Qingdao 266109, China*

Zhe Zhao − *State Key Laboratory of Microbial Technology, Shandong University, Qingdao 266237, China*

Qingsheng Qi − *State Key Laboratory of Microbial Technology, Shandong University, Qingdao 266237, China;* orcid.org/0000-0001-5693-6797

Mo Xian − *CAS Key Lab of Biobased Materials, Qingdao Institute of Bioenergy and Bioprocess Technology, Chinese Academy of Sciences, Qingdao 266101, China*

Complete contact information is available at: https://pubs.acs.org/10.1021/acs.jafc.4c04123

Author Contributions

[⊥]J.C. and L.G. contributed equally to this work.

Funding

This study was financially supported by the National Key Research and Development Program of China (2022YFC2104700), NSFC (22277068, 32370068, 32200082), the Fundamental Research Funds for the Central Universities (2021JCG025), the Young Scholars Program of Shandong University (M.L.), the Distinguished Scholars Program of Shandong University (G.Z.), the Taishan Scholars Program (tstp20231208), and the State Key Laboratory of Microbial Technology (M2022−07, WZCX2021−02, and SKLMTFCP-2023−03).

Notes

The authors declare no competing financial interest.

ACKNOWLEDGMENTS

We thank Jing Zhu, Jingyao Qu, Zhifeng Li, and Guangnan Lin from the Core Facilities for Life and Environmental Sciences, State Key laboratory of Microbial Technology of Shandong University, for assistance in chiral analysis by circular dichroism and data processing.

REFERENCES

(1) Patel, R. N. Biocatalysis: synthesis of chiral intermediates for drugs. *Curr. Opin. Drug Discovery* **2006**, *9* (6), 741−764.

(2) Pollard, D. J.; Woodley, J. M. Biocatalysis for pharmaceutical intermediates: the future is now. *Trends Biotechnol.* **2007**, *25* (2), 66−73.

(3) Jaipuri, F. A.; Jofre, M. F.; Schwarz, K. A.; Pohl, N. L. Microwave-assisted cleavage of Weinreb amide for carboxylate protection in the synthesis of a (*R*)-3-hydroxyalkanoic acid. *Tetrahedron Lett.* **2004**, *45* (21), 4149−4152.

(4) Gao, H. J.; Wu, Q.; Chen, G. Q. Enhanced production of D-(−)-3-hydroxybutyric acid by recombinant *Escherichia coli*. *FEMS Microbiol. Lett.* **2002**, *213* (1), 59−65.

(5) Tokiwa, Y.; Ugwu, C. U. Biotechnological production of (*R*)-3-hydroxybutyric acid monomer. *J. Biotechnol.* **2007**, *132* (3), 264−272.

(6) Fei, P.; Luo, Y.; Lai, N.; Wu, H. Biosynthesis of (*R*)-3-hydroxybutyric acid from syngas-derived acetate in engineered *Escherichia coli*. *Bioresour. Technol.* **2021**, *336*, No. 125323.

(7) Chen, G. Q.; Wu, Q. Microbial production and applications of chiral hydroxyalkanoates. *Appl. Microbiol. Biotechnol.* **2005**, *67* (5), 592−599.

(8) Guevara-Martínez, M.; Perez-Zabaleta, M.; Gustavsson, M.; Quillaguamán, J.; Larsson, G.; van Maris, A. J. A. The role of the acyl-CoA thioesterase ″YciA″ in the production of (*R*)-3-hydroxybutyrate by recombinant *Escherichia coli*. *Appl. Microbiol. Biotechnol.* **2019**, *103* (9), 3693−3704.

(9) Mierziak, J.; Burgberger, M.; Wojtasik, W. 3-Hydroxybutyrate as a metabolite and a signal molecule regulating processes of living organisms. *Biomolecules* **2021**, *11* (3), No. 402.

(10) Tseng, H. C.; Martin, C. H.; Nielsen, D. R.; Prather, K. L. Metabolic engineering of *Escherichia coli* for enhanced production of (*R*)- and (*S*)-3-hydroxybutyrate. *Appl. Environ. Microbiol.* **2009**, *75* (10), 3137−3145.

(11) Reddy, G. V.; Guerrero, A. J. V.New Pheromones and Insect Control Strategies. In *Vitamins & Hormones*; Elsevier, 2010; Vol. *83*, pp 493−519.

(12) Carroll, A. L.; Desai, S. H.; Atsumi, S. J. C. o. i. b. Microbial production of scent and flavor compounds. *Curr. Opin. Biotechnol.* **2016**, *37*, 8−15.

(13) Kawata, Y.; Kawasaki, K.; Shigeri, Y. Efficient secreted production of (*R*)-3-hydroxybutyric acid from living *Halomonas sp.* KM-1 under successive aerobic and microaerobic conditions. *Appl. Microbiol. Biotechnol.* **2012**, *96* (4), 913−920.

(14) Perez-Zabaleta, M.; Guevara-Martínez, M.; Gustavsson, M.; Quillaguamán, J.; Larsson, G.; van Maris, A. J. A. Comparison of engineered *Escherichia coli* AF1000 and BL21 strains for (*R*)-3-hydroxybutyrate production in fed-batch cultivation. *Appl. Microbiol. Biotechnol.* **2019**, *103* (14), 5627−5639.

(15) Roland, K.; Curtiss, R., 3rd; Sizemore, D. Construction and evaluation of a delta *cya* delta *crp Salmonella typhimurium* strain expressing avian pathogenic *Escherichia coli* O78 LPS as a vaccine to prevent airsacculitis in chickens. *Avian Dis.* **1999**, *43* (3), 429−441.

(16) Baba, T.; Ara, T.; Hasegawa, M.; Takai, Y.; Okumura, Y.; Baba, M.; Datsenko, K. A.; Tomita, M.; Wanner, B. L.; Mori, H. Construction of *Escherichia coli* K-12 in-frame, single-gene knockout mutants: the Keio collection. *Mol. Syst. Biol.* **2006**, *2*, No. 2006.0008.

(17) McMahon, M. D.; Prather, K. L. Functional screening and in vitro analysis reveal thioesterases with enhanced substrate specificity profiles that improve short-chain fatty acid production in *Escherichia coli*. *Appl. Environ. Microbiol.* **2014**, *80* (3), 1042−1050.

(18) Clomburg, J. M.; Vick, J. E.; Blankschien, M. D.; Rodríguez-Moyá, M.; Gonzalez, R. A synthetic biology approach to engineer a functional reversal of the *β*-oxidation cycle. *ACS Synth. Biol.* **2012**, *1* (11), 541−554.

(19) Alber, B. E.; Fuchs, G. Propionyl-coenzyme A synthase from *Chloroflexus aurantiacus*, a key enzyme of the 3-hydroxypropionate

cycle for autotrophic CO_2 fixation. *J. Biol. Chem.* **2002**, *277* (14), 12137−12143.
(20) Zhou, Q.; Shi, Z. Y.; Meng, D. C.; Wu, Q.; Chen, J. C.; Chen, G. Q. Production of 3-hydroxypropionate homopolymer and poly(3-hydroxypropionate-co-4-hydroxybutyrate) copolymer by recombinant *Escherichia coli*. *Metab. Eng.* **2011**, *13* (6), 777−785.
(21) Guo, Y.; Oliver, D. J. *E. coli* propionyl-CoA synthetase is regulated in vitro by an intramolecular disulfide bond. *Appl. Biochem. Microbiol.* **2012**, *48* (3), 289−293.
(22) Matsumoto, K.; Tanaka, Y.; Watanabe, T.; Motohashi, R.; Ikeda, K.; Tobitani, K.; Yao, M.; Tanaka, I.; Taguchi, S. Directed evolution and structural analysis of NADPH-dependent Acetoacetyl Coenzyme A (Acetoacetyl-CoA) reductase from *Ralstonia eutropha* reveals two mutations responsible for enhanced kinetics. *Appl. Environ. Microbiol.* **2013**, *79* (19), 6134−6139.
(23) Kim, E. J.; Kim, K. J. Crystal structure and biochemical characterization of PhaA from *Ralstonia eutropha*, a polyhydroxyalkanoate-producing bacterium. *Biochem. Biophys. Res. Commun.* **2014**, *452* (1), 124−129.
(24) Park, J. B. Oxygenase-based whole-cell biocatalysis in organic synthesis. *J. Microbiol. Biotechnol.* **2007**, *17* (3), 379−392.
(25) Zhao, H.; van der Donk, W. A. Regeneration of cofactors for use in biocatalysis. *Curr. Opin. Biotechnol.* **2003**, *14* (6), 583−589.
(26) Lee, W. H.; Kim, M. D.; Jin, Y. S.; Seo, J. H. Engineering of NADPH regenerators in *Escherichia coli* for enhanced biotransformation. *Appl. Microbiol. Biotechnol.* **2013**, *97* (7), 2761−2772.
(27) Xu, J. Z.; Zhang, J. L.; Guo, Y. F.; Jia, Q. D.; Zhang, W. G. Heterologous expression of *Escherichia coli* fructose-1,6-bisphosphatase in *Corynebacterium glutamicum* and evaluating the effect on cell growth and L-lysine production. *Prep. Biochem. Biotechnol.* **2014**, *44* (5), 493−509.
(28) Wendisch, V. F. Amino Acid Biosynthesis − Pathways, Regulation, and Metabolic Engineering. In *The L-lysine Story: From Metabolic Pathways to Industrial Production*; Springer: New York, NY, 2007; pp 39−70.
(29) Sánchez, A. M.; Andrews, J.; Hussein, I.; Bennett, G. N.; Progress, K. Y. S. J. B. Effect of overexpression of a soluble pyridine nucleotide transhydrogenase (UdhA) on the production of poly(3-hydroxybutyrate) in *Escherichia coli*. *Biotechnol. Prog.* **2006**, *22* (2), 420−425.
(30) Sauer, U.; Canonaco, F.; Heri, S.; Perrenoud, A.; Fischer, E. The soluble and membrane-bound transhydrogenases UdhA and PntAB have divergent functions in NADPH metabolism of *Escherichia coli*. *J. Biol. Chem.* **2004**, *279* (8), 6613−6619.
(31) Holm, A. K.; Blank, L. M.; Oldiges, M.; Schmid, A.; Solem, C.; Jensen, P. R.; Vemuri, G. N. Metabolic and transcriptional response to cofactor perturbations in *Escherichia coli*. *J. Biol. Chem.* **2010**, *285* (23), 17498−17506.
(32) Kawai, S.; Mori, S.; Mukai, T.; Hashimoto, W.; Murata, K. Molecular characterization of *Escherichia coli* NAD kinase. *Eur. J. Biochem.* **2001**, *268* (15), 4359−4365.
(33) Li, Z. J.; Cai, L.; Wu, Q.; Chen, G. Q. Overexpression of NAD kinase in recombinant *Escherichia coli* harboring the *phbCAB* operon improves poly(3-hydroxybutyrate) production. *Appl. Microbiol. Biotechnol.* **2009**, *83* (5), 939−947.
(34) Lee, H. C.; Kim, J. S.; Jang, W.; Kim, S. Y. Thymidine production by overexpressing NAD^+ kinase in an *Escherichia coli* recombinant strain. *Biotechnol. Lett.* **2009**, *31* (12), 1929−1936.
(35) Liu, M.; Feng, X.; Ding, Y.; Zhao, G.; Liu, H.; Xian, M. Metabolic engineering of *Escherichia coli* to improve recombinant protein production. *Appl. Microbiol. Biotechnol.* **2015**, *99* (24), 10367−10377.
(36) Peskov, K.; Goryanin, I.; Prank, K.; Tobin, F.; Demin, O. Kinetic modeling of *ace* operon genetic regulation in *Escherichia coli*. *J. Bioinf. Comput. Biol.* **2008**, *06* (5), 933−959.
(37) Liu, M.; Ding, Y. M.; Chen, H. L.; Zhao, Z.; Liu, H. Z.; Xian, M.; Zhao, G. Improving the production of acetyl-CoA-derived chemicals in *Escherichia coli* BL21(DE3) through *iclR* and *arcA* deletion. *BMC Microbiol.* **2017**, *17*, No. 10.
(38) Liu, M.; Yao, L.; Xian, M.; Ding, Y.; Liu, H.; Zhao, G. Erratum to: Deletion of *arcA* increased the production of acetyl-CoA-derived chemicals in recombinant *Escherichia coli*. *Biotechnol. Lett.* **2016**, *38* (4), No. 741.
(39) McKee, A. E.; Rutherford, B. J.; Chivian, D. C.; Baidoo, E. K.; Juminaga, D.; Kuo, D.; Benke, P. I.; Dietrich, J. A.; Ma, S. M.; Arkin, A. P.; Petzold, C. J.; Adams, P. D.; Keasling, J. D.; Chhabra, S. R. Manipulation of the carbon storage regulator system for metabolite remodeling and biofuel production in *Escherichia coli*. *Microb. Cell Fact.* **2012**, *11*, No. 79.
(40) Matsumoto, K.; Okei, T.; Honma, I.; Ooi, T.; Aoki, H.; Taguchi, S. Efficient (*R*)-3-hydroxybutyrate production using acetyl CoA-regenerating pathway catalyzed by coenzyme A transferase. *Appl. Microbiol. Biotechnol.* **2013**, *97* (1), 205−210.
(41) Lee, S. H.; Park, S. J.; Lee, S. Y.; Hong, S. H. Biosynthesis of enantiopure (*S*)-3-hydroxybutyric acid in metabolically engineered *Escherichia coli*. *Appl. Microbiol. Biotechnol.* **2008**, *79* (4), 633−641.
(42) Guo, L.; Liu, M.; Bi, Y.; Qi, Q.; Xian, M.; Zhao, G. Using a synthetic machinery to improve carbon yield with acetylphosphate as the core. *Nat. Commun.* **2023**, *14* (1), No. 5286.
(43) Phue, J. N.; Noronha, S. B.; Hattacharyya, R.; Wolfe, A. J.; Shiloach, J. Glucose metabolism at high density growth of *E. coli* B and *E. coli* K: differences in metabolic pathways are responsible for efficient glucose utilization in *E. coli* B as determined by microarrays and Northern blot analyses. *Biotechnol. Bioeng.* **2005**, *90* (7), 805−820.
(44) Yoon, S. H.; Jeong, H.; Kwon, S. K.; Kim, J. F. Genomics, Biological Features, and Biotechnological Applications of *Escherichia coli* B: "Is B for Better?!". In *Systems Biology and Biotechnology of Escherichia coli*; Springer, 2009; pp 1−17.
(45) Liu, Q.; Ouyang, S. P.; Chung, A.; Wu, Q.; Chen, G. Q. Microbial production of *R*-3-hydroxybutyric acid by recombinant *E. coli* harboring genes of *phbA*, *phbB*, and *tesB*. *Appl. Microbiol. Biotechnol.* **2007**, *76* (4), 811−818.

https://doi.org/10.1021/acs.jafc.4c04123
J. Agric. Food Chem. XXXX, XXX, XXX−XXX